UC Davis

UC Davis Previously Published Works

Title

Living in a trash can: turbulent convective flows impair Drosophila flight performance

Permalink

https://escholarship.org/uc/item/2661c463

Journal

Journal of The Royal Society Interface, 15(147)

ISSN

1742-5689

Authors

Ortega-Jiménez, Victor Manuel
Combes, Stacey A

Publication Date

2018-10-01

DOI

10.1098/rsif.2018.0636

Peer reviewed

eScholarship.org Powered by the California Digital Library
University of California

INTERFACE

rsif.royalsocietypublishing.org

Research

Cite this article: Ortega-Jiménez VM, Combes SA. 2018 Living in a trash can: turbulent convective flows impair *Drosophila* flight performance. *J. R. Soc. Interface* **15**: 20180636. http://dx.doi.org/10.1098/rsif.2018.0636

Received: 20 August 2018
Accepted: 1 October 2018

Subject Category:
Life Sciences–Physics interface

Subject Areas:
biomechanics

Keywords:
thermal convection, turbulence, insect flight

Author for correspondence:
Victor Manuel Ortega-Jiménez
e-mail: ornithopterus@gmail.com

Electronic supplementary material is available online at https://dx.doi.org/10.6084/m9.figshare.c.4260704.

THE ROYAL SOCIETY PUBLISHING

Living in a trash can: turbulent convective flows impair *Drosophila* flight performance

Victor Manuel Ortega-Jiménez and Stacey A. Combes

Department of Neurobiology, Physiology, and Behavior, University of California, Davis, CA, USA

VMO-J, 0000-0003-0024-5086; SAC, 0000-0003-1586-6459

Turbulent flows associated with thermal convection are common in areas where the ground is heated by solar radiation, fermentation or other processes. However, it is unknown how these flow instabilities affect the locomotion of small insects, like fruit flies, that inhabit deserts and urban landscapes where surface temperatures can reach extreme values. We quantified flight performance of fruit flies (*Drosophila melanogaster*) traversing a chamber through still air and turbulent Rayleigh–Bénard convection cells produced by a vertical temperature gradient. A total of 34% of individuals were unable to reach the end of the chamber in convection, although peak flow speeds were modest relative to typical outdoor airflow. Individuals that were successful in convection were faster fliers and had larger wing areas than those that failed. All flies displayed higher pitch angles and lower mean flight speeds in convection. Successful individuals took longer to cross the chamber in convection, due to lower flight speeds and greater path sinuosity. All individuals displayed higher flapping frequencies in convection, and successful individuals also reduced stroke amplitude. Our results suggest that thermal convection poses a significant challenge for small fliers, resulting in increased travel times and energetic costs, or in some cases precluding insects from traversing these environments entirely.

1. Introduction

Thermal convection is a universal phenomenon that occurs at a vast range of spatio-temporal scales, affecting atmospheric circulation and weather patterns as well as flow within sub-millimetre fluid films. This flow instability is driven by a temperature gradient between a surface and the surrounding fluid, and it depends on gravity, buoyancy of the heated fluid and thermal diffusion forces (with instability of the fluid quantified by the Raleigh number, *Ra*) [1]. At low to moderate surface temperatures, the resulting flow typically remains laminar, with flows rising from the surface and then circling back down to form smooth, rounded flow 'cells'—but, when surface temperatures reach extreme values ($Ra > 10^6$), flow within these cells becomes unsteady and turbulent [2,3]. In natural habitats, solar radiation, in conjunction with physical surface properties and weather conditions (e.g. no wind), plays the most important role in driving intense convection processes. The maximal ground temperatures in deserts and urban areas (with concrete/asphalt surfaces) can range between 70°C and 100°C [4–6], and fermentation and/or decomposition can produce similar temperatures in areas containing garbage or fallen fruit. Thus, for insects such as fruit flies that live and fly near surfaces heated by various processes (i.e. solar radiation, fermentation and decomposition), thermal convection may represent a significant everyday challenge.

Over the past decade, a number of studies have examined animal flight performance in perturbed flow environments, including von Kármán vortex streets [7–9], whirlwinds [10], homogeneous turbulent airflows [11–13] and wind gusts [14], but the effects of thermal convective flows on animal flight performance have not been tested experimentally. Soaring and migrating animals are

© 2018 The Author(s) Published by the Royal Society. All rights reserved.

well known for using large, vertical thermals that result from convection processes [15–17], presumably to reduce flight costs; however, the effects of convection on millimetre-sized animal fliers, which may encounter convective flows associated with heated surfaces more frequently than larger animals, have not been addressed.

Here, we analysed the effects of Rayleigh–Bénard convection cells on the flight kinematics and control of fruit flies. We used the common fruit fly (*Drosophila melanogaster*) because this species is capable of travelling long distances in the desert to colonize oases (for a review see [18]), and because they are common inhabitants of trash cans and dumpsites in human cities, where the process of solar radiation (combined with bacterial processes, in some cases) can lead to extreme surface temperatures and thus induce thermal convection. We hypothesize that fruit flies flying through Rayleigh–Bénard cells will be challenged by the vertical shear and dynamic variable flows, and this will be reflected by changes in their flight trajectory and in the total time required to traverse a flight chamber, in comparison with control flights performed in still air.

2. Material and methods

2.1. Sampled insects

We performed repeated measures testing on 32 individual fruit flies (*Drosophila melanogaster*) from a laboratory colony established from wild founders collected near the University of California, Davis. The colony was kept in a mesh cage (30 × 30 × 30 cm) with food (bananas), water and salt available ad libitum, and with natural lighting to provide a normal daylight cycle (9 : 30 : 14 : 30 h). Single individuals from the mesh box were collected for experimental testing using an LED ultraviolet flashlight (Black-light Master, 390 nm, model 302490) for attraction and a 10 mm syringe for capture; only individuals that were strongly attracted to the UV light were used for experiments. Handling of flies was minimized before flight experiments to avoid interfering with flight motivation and performance; as a result, sex sample distribution could not be controlled, and the testing group ultimately contained seven males and 25 females. After flight tests, each individual was frozen and photographed to measure body length (l_b) and wing area (S) using WingImageProcessor v.1.1 for Matlab (available at https://www.unc.edu/~thedrick/software3.html), and sex was determined using a dissecting scope.

2.2. Flight chamber

Each sampled insect was kept in total darkness for approximately 10 min before being transported to the flight chamber (22 × 12 × 8 cm). The side walls of the chamber were made of clear, 1 mm thick Plexiglas sheets, while the bottom and upper walls were made of 1 mm thick stainless steel sheets. The end walls of the chamber were each perforated with a 0.5 cm hole, with one opening used to release the insect into the chamber via the syringe and the other to recapture the insect in a small plastic vial after it flew across the chamber. To produce a strong, positive phototaxis during flights, we mounted a UV lamp (Exo-Terra Reptile UVB150, 26 W, 0.34 mW cm^{-2}) facing the wall where the vial for re-capturing flies was attached (figure 1*a*).

Rayleigh–Bénard convection cells were produced in the chamber by heating the floor with an infrared lamp (125 W) placed 10 cm below the bottom steel plate and cooling the ceiling with refrigerant gels placed above the top plate (figure 1*a*). The temperatures of the bottom and top plates were $T_b = 70^\circ$C and $T_t = 4^\circ$C, respectively. We calculated the Prandtl number as $Pr = \upsilon\kappa^{-1}$, where υ is the kinematic viscosity and κ the thermal diffusivity of air. Rayleigh number was calculated as $Ra = \alpha g(T_b - T_t)d_H^3\upsilon^{-1}\kappa^{-1}$, where α is the thermal expansion coefficient, g the acceleration of gravity and d_H the distance between the upper and lower plates [1].

2.3. Flow description and temperature profile

We characterized the velocity field of the turbulent convective flow in the flight chamber using a digital particle image velocimetry (DPIV) method when no insects were present. A laser pointer (JD-303, 532 nm, 5 mW, Class IIB laser) with a glass stir rod mounted at its tip was used to produce a two-dimensional vertical laser screen (approx. 2 mm thickness) and the flow was seeded with lycopodium particles (approx. 30 µm; figure 1*b*). We used a Phantom camera (model V611) to film the particles moving through the projected laser sheet at 1000 frames/s after generating a temperature gradient between the top and bottom plates of the chamber. We used 700 video frames ($\tau = 0.7$ s) to calculate a cross-correlation of image pairs with an interrogation window from 64 pixels^2 to 32 pixels^2, excluding those vectors with standard deviation greater than 4, to resolve the average velocity field using PIVlab in Matlab [19]. We calculated the turbulence intensity I_t (i.e. the ratio between the root-mean-square of velocity fluctuations and the mean velocity) at three points along the midline of the chamber (green asterisks in figure 1), using the velocity fields from the PIV analysis.

We measured the average temperature profile of the chamber using a k-type thermometer (MN Measurement Instruments, model DM6801, accuracy of 0.1°C) with a thermocouple wire probe. This isolated wire with a sensitive tip was introduced into the chamber and temperatures were collected (after readings stabilized) approximately every 2.5 cm throughout the vertical plane of the chamber (i.e. from top to bottom, along the midline of the flight chamber). We photographed the position of the wire tip during each measurement and calculated its Cartesian coordinates using DLTdv5 in Matlab [20]. With these data, we created an average temperature profile map along the vertical plane of the chamber. It is worth noting, however, that the thermometer used had a relatively low sampling rate (2.5 Hz) in comparison to our flow sampling (1000 Hz), which limits the details of instantaneous temperature changes. Ambient temperature in the room (and within the chamber in still-air conditions) was 21°C.

2.4. Video recording

Each individual was filmed while flying along the chamber through still air (non-perturbed flow) and then through convective flow, from the point of release to the opposite wall, or to wherever flight ceased if the fly failed to reach the opposite wall. We were unable to randomize the order of these treatments because flies that failed to reach the opposite wall in the convective flow condition and landed instead on the floor were typically killed by the high temperature of the aluminium plate. However, to verify that fatigue was not responsible for any flight differences seen in convective flow, we performed an additional (third) flight trial in still air for five individuals that successfully completed trials in convection, and compared results of this trial to the first still-air control. After each flight across the chamber, flies were kept inside the container used to capture them, in the dark, for approximately 10 min before flying across the chamber in the next flow condition. We filmed individual flights at 3500 frames/s using two high-speed cameras (Phantom V611) placed approximately perpendicular to the vertical plane of the chamber, with an angle of approximately 40° between the cameras. An LED infrared bulb (Feit electric, 30 W) with a plastic diffuser was used to illuminate the rear wall of the chamber for visualizing the fly's body and wings.

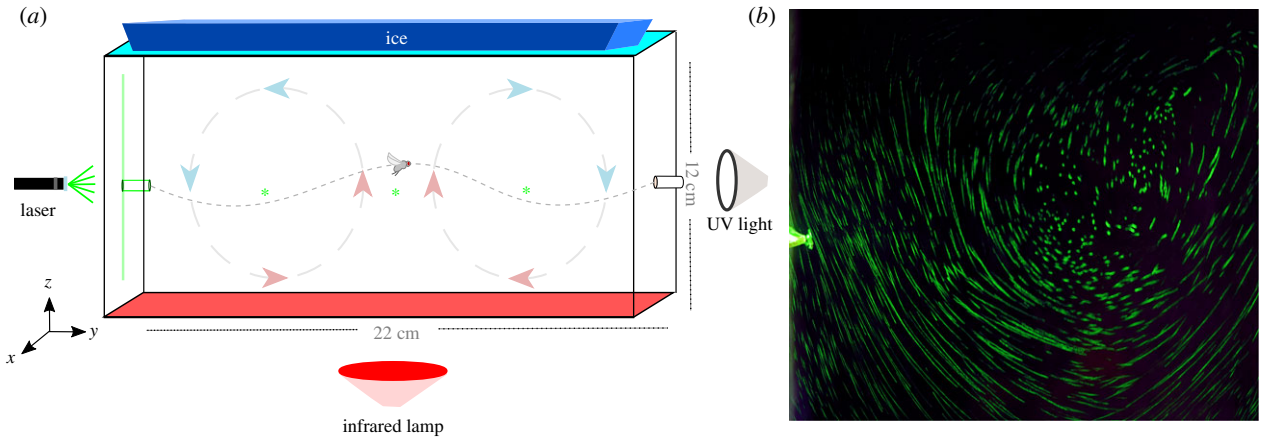

Figure 1. (*a,b*) Experimental set-up for testing *Drosophila* flight performance in still and thermal convective flow. (*a*) Illustration of flight chamber and method used to produce Rayleigh–Bénard convection cells. (*b*) Image of a fly just before take-off (left side, on syringe tip), with flow particles illuminated to show the left half of the convective flow field. Note that actual flight trials were performed without the laser or particles, which were used only to calculate the average velocity field using DPIV. Green asterisks represent the point where turbulence intensity was measured from PIV analyses.

We analysed films from each individual ($n = 32$) in both convection and still-air conditions, as well as a third flight trial (post-convection control trial) in five individuals, resulting in a total of 69 individual flights and approximately 345 000 digitized frames. For each flight trial, we digitized the position of the front of the head and the tip of the abdomen during each frame from take-off to landing. We also digitized the position of the right wing-base and tip over five flapping cycles during the middle of the filmed sequence. The position of each digitized point from the two cameras was transformed to Cartesian coordinates using a direct linear transformation method [20] and smoothed using an MSE quintic spline function [21]. The first derivative of three-dimensional head position was used to calculate instantaneous speed (u_i) and these data were then averaged over the entire sequence to calculate mean flight speed (u_m). Travel time (t_t) was calculated by dividing the total number of frames from take-off to landing by the frame rate. Path sinuosity (Si) was calculated by summing the three-dimensional distance between successive points to obtain the total length of the flight path and dividing by the linear distance between the take-off and landing positions (figure 2*a*). Reynolds number was calculated as $Re = u_m l_b/\nu$, where ν is the kinematic viscosity of air.

The vector angle formed by the head and abdomen with respect to the horizontal plane was used to calculate body pitch (β; figure 2*b*). Wing stroke amplitude (Φ) was extracted from the instantaneous angle of the vector formed between the wing tip and its base, and wingbeat frequency (n) was calculated by dividing the frame rate by the number of frames in each wingbeat cycle.

2.5. Statistics

During the experiments, 21 individuals completed flights across the chamber in convective flow (success group) while the remaining 11 individuals failed to reach the opposite wall in this flow condition (failure group). We used a binary logistic regression to examine the effects of body length, wing area, sex and mean flight speed in still air on the likelihood of failure versus success in convective flow. Body length, wing area, sex and mean flight speed in still air were not collinear ($VIF^{0.5} < 2$ for all contrasts, where VIF is the variance inflation factor).

We next examined relationships among flight performance variables. To determine whether travel time across the chamber depends on mean flight speed along the flight path and/or path sinuosity, we performed stepwise multiple linear regression on trials in still air (all individuals) and in convective flow (success/failure groups analysed separately, since failed individuals did not reach the same landing position as successful ones). Similarly, to determine whether mean flight velocity depends on body morphology and/or kinematics (body length, wing area, pitch angle, flapping frequency and stroke amplitude), we performed stepwise multiple linear regression on trials in still air and in convective flow (with all individuals grouped together).

To evaluate changes in flight performance between still-air and convective flow conditions, we performed paired *t*-tests (or paired Wilcoxon signed-rank tests, where assumptions of *t*-tests were not met) on flight and wing kinematic variables (t_t, Si, u_m, β, n and Φ), evaluating all individuals together and also evaluating success/failure groups separately. We also performed paired *t*-tests comparing these variables in individuals for which we collected still-air trials both before and after the convection trial ($N = 5$), to determine whether fatigue led to consistent changes in flight performance.

To determine whether there was a difference in how flies in the success versus failure group altered their flight kinematics in convective flow, we calculated each individual's change in flight kinematics (t_t, Si, u_m, β, n and Φ) from still air to convective flow, and then performed unpaired *t*-tests comparing the mean change in variables between the success and failure groups. We also performed unpaired *t*-tests of all morphological and kinematic variables to compare males versus females, in both still air and convection conditions. For the above tests, function transformations ($\log f(x)$ or $f(x)^n$) were applied to variables when needed, and all variables used for *t*-tests fulfilled requirements of homogeneity of variance and normality. Data are presented as means $\pm$ one standard deviation. All statistical analyses were performed in R v. 3.4.1 [22].

3. Results

3.1. Flow and temperature characterization

When a vertical temperature gradient was applied, flow in the flight chamber was characterized by two horizontal counter-rotating vortices, with Prandtl (Pr) and Rayleigh (Ra) numbers of 0.7 and 1×10^7, respectively. The counter-rotating vortices were highly unsteady and turbulent, with small eddies appearing and decaying frequently (electronic supplementary material, video S1). Maximal flow speeds (approx. 0.3 m s^{-1}) were found in the updraft plumes in-between the vortices, at the middle of the chamber (figure 3*a*), and vorticity values ranged from $+40$ s^{-1} to -30 s^{-1} (electronic

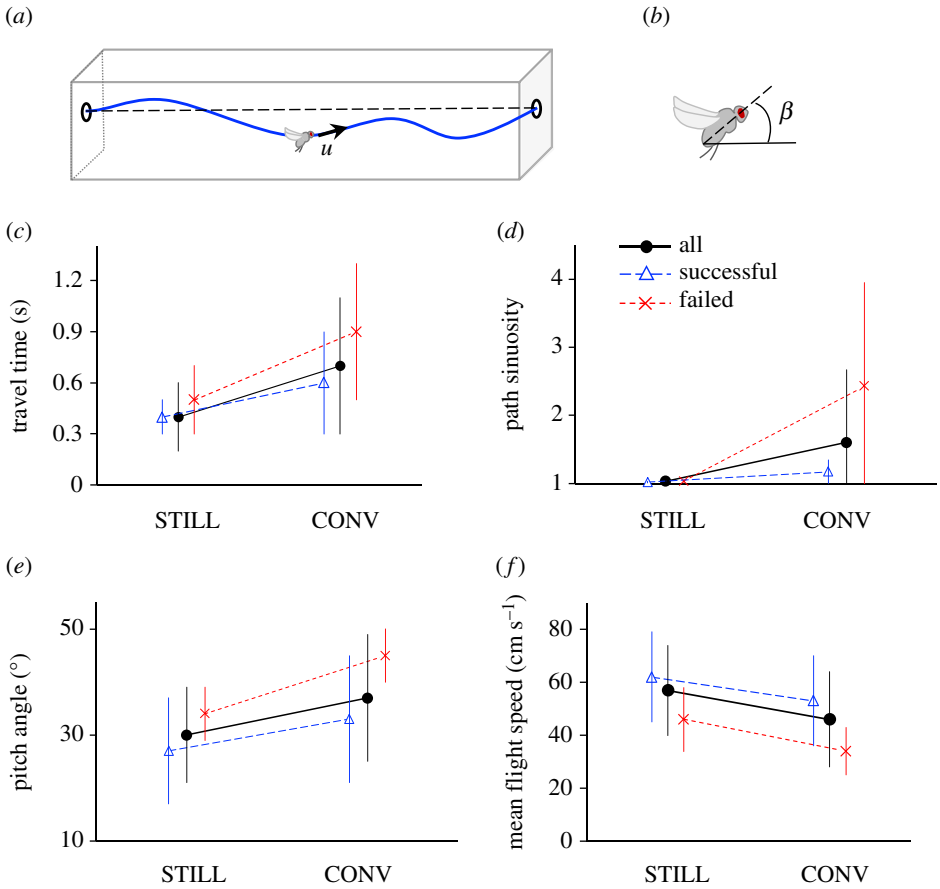

Figure 2. Flight performance of fruit flies in still air and convective flow. (*a*) Measured variables include travel time across the flight chamber and path sinuosity, calculated as the total distance of the flight path (solid line) divided by the linear distance from take-off to landing (dashed line). Instantaneous velocity along the three-dimensional flight path (*u*) was measured throughout the flight sequence and averaged to obtain mean flight speed. (*b*) Pitch angle of the body relative to the horizontal was measured in each video frame and averaged over the entire flight sequence. (*c*) Travel time, (*d*) path sinuosity, (*e*) mean pitch angle and (*f*) mean flight speed in still air (STILL) and convective flow (CONV) are shown for all individuals grouped together ($N = 32$, circles), for individuals that successfully crossed the flight chamber in convection ($N = 21$, triangles), and for individuals that failed to cross the chamber in convection ($N = 11$, crosses). Data represent means $\pm$ one standard deviation. All groups displayed a significant increase in travel time, path sinuosity, and pitch angle, and a decrease in mean flight speed in convective flow ($p < 0.05$, see text for details). (Online version in colour.)

supplementary material, figure SA). Turbulence intensity I_t at the three points sampled was 28% (left eddy), 24% (uprising zone; see electronic supplementary material, figure SE) and 29% (right eddy).

The Reynolds number of flies flying in the chamber was approximately 10^2. Average temperature in the chamber was 35°C (60% higher than the ambient/still air temperature of 21°C), with a range of 20°C to 50°C (figure 3*b*).

3.2. Flight kinematics

We found that 34% of flies failed to reach the opposite wall under convection. These individuals started to lose flight control and displayed more erratic flight paths after passing through the convection updraft in the middle of the chamber (figure 4*b*). A binary logistic regression model testing the effects of body length, wing area, sex and mean flight speed in still air on the likelihood of success versus failure was statistically significant ($\chi^2_4 = 15.5$, $p < 0.01$). The model explained 53% (Nagerlkerke R^2) of the variance in trial outcome and correctly classified 78% of cases. Both higher wing areas ($p = 0.043$) and faster flight speeds in still air ($p = 0.018$) were associated with an increased likelihood of successfully completing flights in convection (electronic supplementary material, figure SB).

Stepwise multiple linear regression analysis indicated that travel time across the chamber in still air was a function of mean flight speed ($F_{2,30} = 88$, $R^2 = 0.74$, $p < 0.001$) but not path sinuosity (likely because all paths were fairly straight in still air). However, for the successful group in convection, travel time was a function of both path sinuosity and mean flight speed ($F_{2,18} = 63$, $R^2 = 0.86$, $p < 0.001$; u_m $p < 0.001$, Si $p < 0.001$) (electronic supplementary material, figure SC), with travel time increasing as path sinuosity rises and mean flight speed declines. For the failed group in convection, landing spots were highly variable and travel time was independent of u_m and Si ($F_{2,8} = 0.7$, $R^2 = -0.1$, $p = 0.54$). Multiple regression analysis of factors affecting mean flight speed indicated that speed depends only on body pitch, in both still air ($F_{2,30} = 148$, $R^2 = 0.83$, $p < 0.001$) and convection ($F_{2,30} = 126$, $R^2 = 0.8$, $p < 0.001$), with body length, wing area, flapping frequency and stroke amplitude being eliminated as insignificant factors (electronic supplementary material, figure SD).

All flies displayed altered flight performance in convective flow, with significantly longer travel times (Wilcoxon's test, $V = 72$, $p < 0.01$), higher path sinuosity (Wilcoxon's test, $V = 0$, $p < 0.01$; figure 4; electronic supplementary material, video S2), higher pitch angles ($t_{31} = -4.2$, $p < 0.01$) and lower mean flight speeds ($t_{31} = 3.7$, $p < 0.01$) in comparison with still-air conditions (figure 2). Flies also displayed

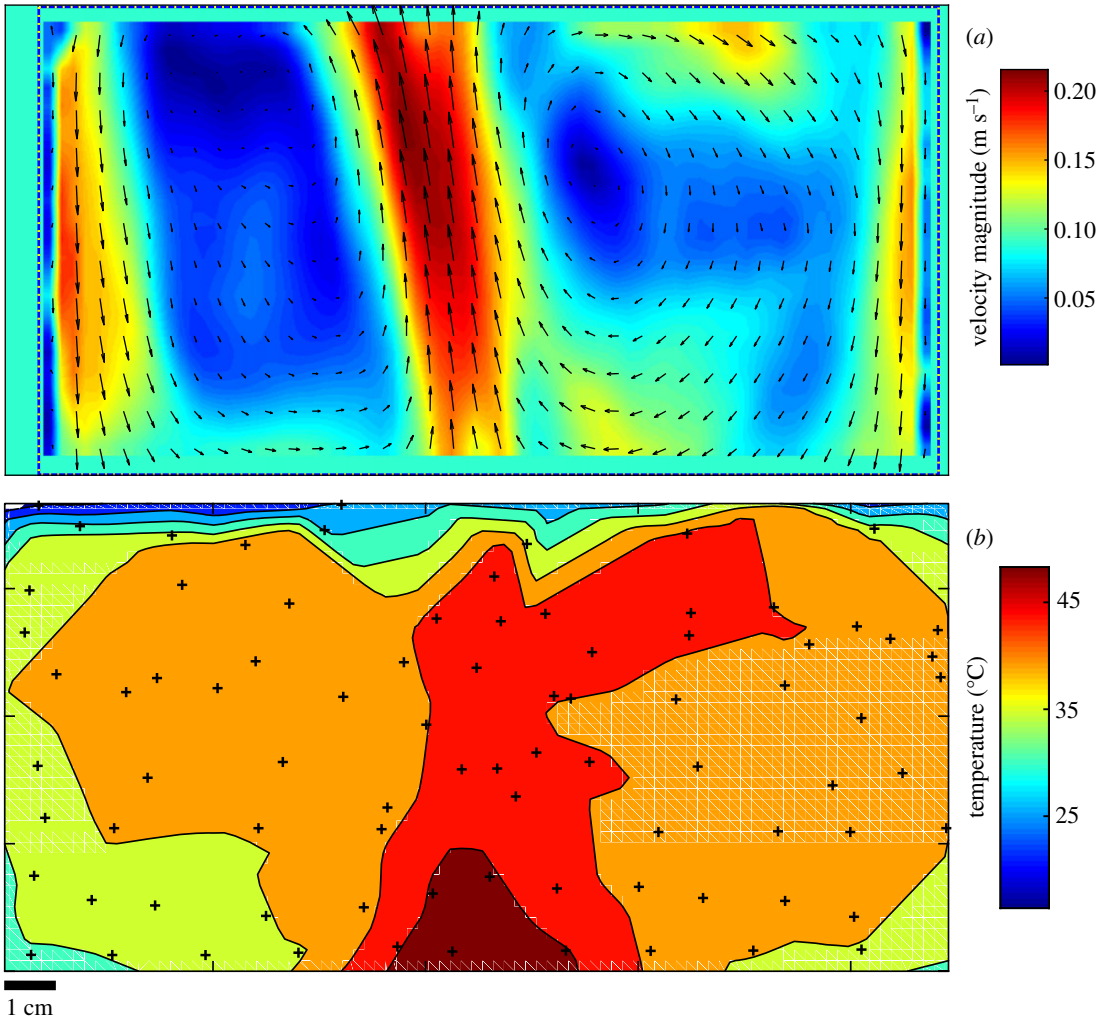

Figure 3. Velocity field (*a*) and temperature profile (*b*) resulting from Rayleigh–Bénard convection cells in the flight chamber.

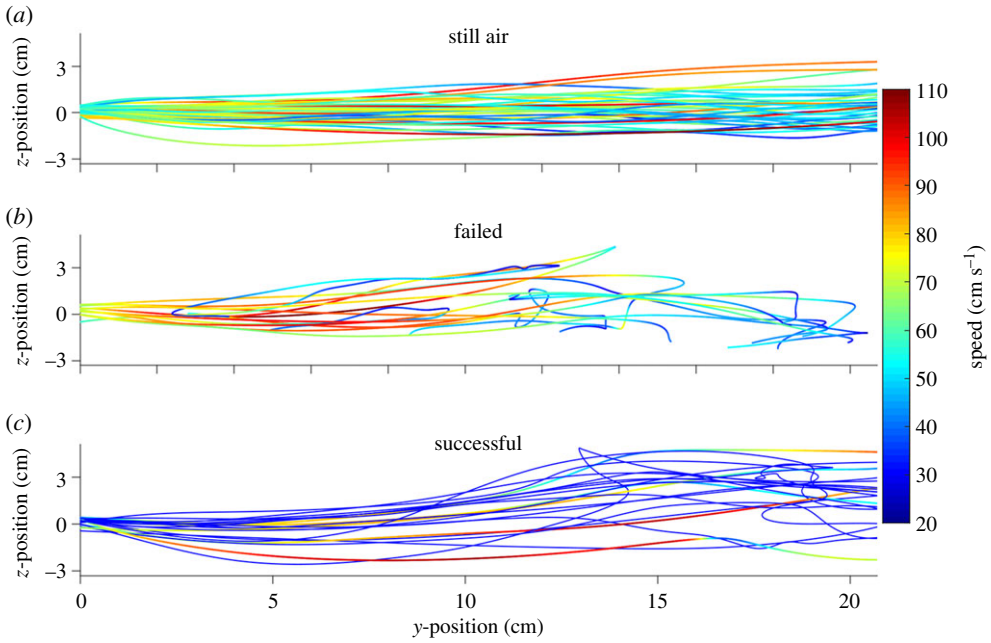

Figure 4. Vertical position and flight velocity (colour bar) along the length of the flight chamber, for fruit flies moving in still air and convection conditions. Flight path of flies in still air is shown in the top (*a*), flies that failed to complete convection trials in the middle (*b*), and flies that successfully completed trials in convective flow in the bottom (*c*). Sample sizes shown are $N = 37$ for still air (32 individuals plus extra control trials after convection on 5 of these individuals), $N = 11$ individuals for the failed convection group, and $N = 21$ individuals for the successful convection group.

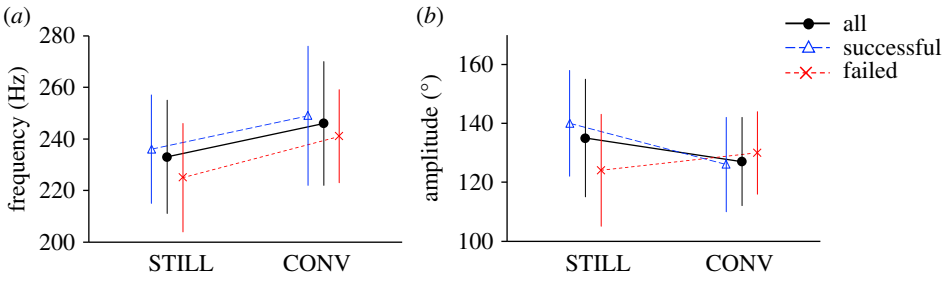

Figure 5. Wing kinematics of fruit flies in still air and convective flow, measured over five wingbeats in the middle of the flight sequence. (*a*) Flapping frequency and (*b*) stroke amplitude in still air (STILL) and convective flow (CONV) are shown for all individuals grouped together ($N = 32$, circles), for individuals that successfully crossed the flight chamber in convection ($N = 21$, triangles), and for individuals that failed to cross the chamber in convection ($N = 11$, crosses). Data represent means $\pm$ one standard deviation. All groups displayed a significant increase in flapping frequency in convective flow ($p < 0.05$, see text for details). Successful individuals displayed a significant decrease in stroke amplitude in convective flow ($p < 0.05$), whereas failed individuals (and all individuals together) did not display any difference in amplitude. (Online version in colour.)

higher flapping frequencies in convection ($t_{31} = -5.7$, $p < 0.01$), but no significant change in stroke amplitude (figure 5). When success and failure groups were analysed separately, similar results were obtained for significant differences between still-air and convection conditions in travel time (failure: $t_{10} = -2.8$, $p < 0.05$, success: $V = 32$, $p < 0.01$), path sinuosity (failure: Wilcoxon's test, $V = 0$, $p < 0.001$, success: $V = 0$, $p < 0.001$), pitch angle (failure: $t_{10} = -5.1$, $p < 0.001$, success: $t_{20} = -2.3$, $p < 0.05$), mean flight speed (failure: $t_{10} = 2.9$, $p < 0.05$, success: $V = 2.6$, $p < 0.05$) and flapping frequency (failure: $t_{10} = -4.8$, $p < 0.001$, success: $t_{20} = -4$, $p < 0.001$; figures 2 and 5). Successful flies also displayed significantly lower stroke amplitudes ($t_{20} = -2.8$, $p < 0.05$) when flying in convection as compared to still air (figure 5; electronic supplementary material, table S1), whereas failed flies displayed no difference in amplitude.

We found no significant differences between successful and failed flies in how individuals adjusted their flight kinematics from still air to convection, with the exception of stroke amplitude ($t_{22.2} = -2.4$, $p < 0.05$), where successful flies reduced amplitude in convection but failed flies did not, and path sinuosity (Wilcoxon's test, $V = 32$, $p < 0.01$), where failed flies displayed a significantly larger increase in path sinuosity in convective flow.

We found no significant differences in morphology or flight performance between males and females, in either still air or convective flow ($p > 0.5$ for all variables; electronic supplementary material, table S2). Similarly, we found no significant, directional differences in flight performance due to fatigue/testing order, in individuals tested in still air both before and after convection trials ($p > 0.5$ for all variables; electronic supplementary material, table S3).

Finally, we observed that although most individuals displayed longer travel times and lower mean flight speeds in convection, five of the 21 successful individuals actually displayed shorter travel times (18% shorter on average) and higher mean flight speeds (27% higher on average) in convective flow as compared to still air (electronic supplementary material, video S2).

4. Discussion

Thermal convection is a major flow disruptor in the atmosphere, inducing air motion from local to planetary scales, and generating some of the most dramatic weather conditions experienced by small animals, such as tornadoes and thunderstorms. During fair weather, surfaces exposed to solar radiation (e.g. soil, rocks, vegetation, and even vertebrate fur, scales or feathers) can reach temperatures equivalent to the boiling point of water [4,23], and the surfaces of man-made materials (e.g. glass, metal, plastics, blacktop and concrete) can reach even higher temperatures, which can generate intense convective plumes and rolls. Thus, diurnal insects that routinely move over such solar-heated surfaces must overcome the challenges associated with thermal convection.

Here, we demonstrated that turbulent convection cells generally have a negative effect on the flight control and performance of common fruit flies. More than a third of the individuals tested in convective flow were unable to maintain a controlled flight trajectory and fell to the ground before reaching their landing target, despite the fact that peak flow speeds were modest in comparison to measurements of typical outdoor airflow (e.g. mean wind speeds of 1.0 m s^{-1} during mild, summer conditions [24]). It is worth noting that the induced flow speeds of up to 0.3 m s^{-1} in this experiment (electronic supplementary material, video S4) correspond to approximately 50% of the average flight speed displayed by flies during still air conditions, but these are still well below maximal flight speeds of fruit flies reported in the literature [25]. Flies that were able to negotiate the perturbed flow had longer travel times due to greater path sinuosity and lower mean flight velocity (figure 2), despite displaying higher flapping frequencies (figure 5). These results suggest an increased energetic cost associated with flying through convective flows, for the individuals that are capable of traversing these regions.

Although some narrow areas of the flight chamber were near the thermal lethal limits of *Drosophila melanogaster*, especially close to the chamber's bottom (CT_{max} generally ranges from approx. 39.5 to 40.5°C, depending on developmental history [26]), several lines of evidence suggest that the reduced flight performance we observed was due to the aerodynamic rather than the thermal environment. Flies traversed the flight chamber very quickly, generally in less than 1 s, which is far shorter than the time scale over which behavioural effects associated with CT_{max} are normally observed (i.e. approx. 1 min or more). Thus, flies likely crossed the chamber before their bodies had time to equilibrate to the external thermal environment in the convection condition. In addition, several of our observations point to an aerodynamic (rather than thermal) challenge as the

underlying cause of the flight performance declines, including consistent changes in body pitch angle and mean flight speed in convective flow (which would not be expected to result from temperature changes alone), as well as the significant influence of wing area and mean flight speed (but not body length) on the likelihood of individuals being able to successfully complete flights in convection. In addition, our results on turbulence intensity during convection conditions indicate that extreme changes in the trajectory of some flies (figure 4) are associated with zones where turbulence is high, yet average flow speeds and temperatures are modest (i.e. first and third positions sampled, centre of left and right eddies; figure 1*a*). This suggests that instantaneous changes in flow velocity and turbulence have a more significant effect on flight performance than time-averaged flow velocity or instantaneous temperature. Despite these lines of evidence pointing to the overriding influence of aerodynamic conditions on flight performance, thermal effects cannot be entirely discounted without a detailed study focusing on the effects of transient thermal stress (in the absence of external, aerodynamic flows) at extreme temperatures.

Although it is not possible to directly compare our results to previous studies of animal flight in unsteady flows due to the differences in flow dynamics, our results generally agree with previous findings that environmental flow perturbations typically impair the flight performance of animals. These studies indicate that maximal flight speeds of moths [7], bees [11] and hummingbirds [8] are lower in perturbed flow environments than in laminar flows. Furthermore, perturbed flows are associated with instabilities in yaw and/or roll orientation in all three species [7–9], and the severity of rotational instabilities appears to be vortex-size dependent. Vortices close to the size of the wing span have been shown to present a greater challenge than smaller perturbations, likely because when multiple small vortices rotating in different directions interact with the body and wings at the same time, one vortex may partially counteract the destabilizing effects of another one. In contrast, incoming vortices that are as large as or larger than body size tend to interact with the entire animal (body and wings) at once, and thus they can disrupt the animal's attitude at each encounter, with detrimental effects on flight control and energetics (see [27]). Flow in the current study was turbulent and unpredictable (in contrast to the previous studies employing structured von Kármán vortex streets), and PIV could not be performed during trials with fruit flies present; thus, we could not calculate the exact size of vortices encountered by fruit flies relative to their body size. However, PIV analysis of the empty chamber suggests that vortices in the convection condition were substantially larger than fruit fly body length. The only experimental test so far of the effects of vortex systems substantially larger than body size on animal fliers was a study in which moths were challenged to continue hover-feeding in the centre of tornado-like vortices. Moths were able to overcome the most intense whirlwind condition tested (transverse speed = 1.2 m s^{-1} and *Re* approx. 10^3), producing a yaw rate up to 550° s^{-1} [10], but they could only maintain stable flight for a few seconds before losing control and falling to the ground. Similarly, it appears that the high vorticity (up to 40 s^{-1}) found in convection conditions contributed to reduced flight performance of fruit flies in convection. Thus, it seems that regardless of the details of the flow dynamics (i.e. von Kármán vortex shedding, fully mixed turbulence, whirlwinds or convection cells) animal fliers generally experience degraded flight performance in unsteady turbulent flow.

Our study also revealed that convective flows do not affect all individuals equally; faster-flying individuals with larger wings were more likely to be able to successfully traverse the flight chamber in the presence of convection cells (electronic supplementary material, figure SB). This is not surprising, because lift production depends on both variables ($L \propto u^2 S$), and thus flies with the capacity to produce more lift are more capable of overcoming the challenges imposed by unsteady, external flows. Whereas vertebrate fliers can modify wing area at will by bending or extending their forelimbs in response to flight requirements [28], most insects can actively modify wing area only slightly, if at all. Thus, our results indicate that individuals possessing larger fixed-wing areas (not necessarily those with longer body lengths), and who fly at lower body angles and higher flight speeds likely have an advantage in overcoming perturbed flow environments. Although female fruit flies are generally larger than males, we did not find any significant effect of sex on our results. Similar proportions of males and females were able to fly in convective flow, with 71% of males and 64% of females successfully crossing the chamber in this condition. However, because of the difference in sample sizes (seven males versus 25 females) our statistical results concerning the effects of sex may be underpowered.

Upon encountering convective flow, all flies (both successful and failed) responded by increasing their pitch angle and decreasing mean flight speed (figure 2*e*,*f*), as well by increasing the flapping frequency of their wings, by 11% on average (figure 5*a*). We suggest that this increased frequency could serve to improve flight control, especially in the region at the middle of the chamber where an uprising plume dominates and presents the fastest flow speeds (figure 3*a*). Elevated flapping frequency has previously been proposed to enhance control authority, by reducing the time between wing strokes and thus the delay in updating control input to the wings [29], and to reduce the impact of random, turbulent flow perturbations on force production by flapping wings [30]. In agreement with our results, hummingbirds and moths flying in varied vortex shedding conditions increase their stroke frequency approximately 10% as compared to when flying in laminar flows at the same speed [7,8], and bumblebees flying in fully mixed turbulence at higher speeds increase their frequency by approximately 3% [24].

Despite its potential benefits in terms of improved control, increasing flapping frequency likely also increases the energetic cost of flight for fruit flies, due to its strong contribution to inertial power requirements [31]. Successful individuals flying in convection cells significantly lowered their stroke amplitude along with increasing flapping frequency, whereas failed individuals increased frequency without lowering amplitude. This further suggests that individuals that failed to maintain flight in convective flow were challenged in terms of lift production, whereas successful flies were able to lower stroke amplitude to compensate somewhat for their increased flapping frequency. Presumably, failed individuals who raised their flapping frequency without adjusting amplitude produced more total force, and production of elevated flight forces has been shown to reduce manoeuvrability in fruit flies [32]. This may have further challenged the stability of these individuals by

reducing their capacity to respond to sudden perturbations via asymmetric force production.

In contrast to the studies discussed above concerning the negative impacts of unsteady flows on animal flight performance, several previous studies have shown that under certain circumstances, animals can actually take advantage of vortex shedding to improve locomotory performance and/or reduce energetic costs. For example, fish can reduce their muscular activity by synchronizing swimming motions to a von Kármán vortex street shed by an upstream object [33], and ibises flying in formation can make use of the wake produced by the next bird upstream to reduce their induced drag [34]. Similarly, it has been shown that hovering insects can improve lift production by re-capturing the wake produced by one half-stroke during the next [35]. In this study, we observed that five individuals (24% of successful flies) displayed a lower travel time ($t_4 = 3.5$, $p = 0.02$), higher mean flight speed ($t_4 = -4.1$, $p = 0.015$) and higher wingbeat frequency ($t_4 = -3.8$, $p = 0.019$) in convection as compared to still air, but without changing either their pitch orientation ($t_4 = 1.5$, $p > 0.05$) or stroke amplitude ($t_4 = 0.9$, $p > 0.05$) (electronic supplementary material, video S2). These individuals tended to follow a curved path resembling the path of flow produced by the convection vortices. A flow visualization of a fly moving through convection suggests that under certain conditions flies can follow or 'ride' external flow perturbations without losing stability, and possibly improve their flight performance, even beyond that seen in still air (electronic supplementary material, video S3). Because the sample size is so small, this observation must be viewed with caution, but it suggests interesting avenues for future exploration.

Convection is a fundamental process in aeroecology because it determines the distribution of millimetre-sized organisms in the atmosphere, specifically below the convective boundary layer. Radar measurements indicate that small insects, such as aphids, have a diurnal vertical distribution (approx. 10^3 m of height) in the troposphere associated with convection, and particularly with turbulent rising plumes and rolls [36,37]. Owing to the low resolution of radar, it is difficult to determine from these studies whether these tiny fliers have the capacity to actively counteract updrafts produced by convection, or if they are simply moved passively by these flows [37]. Our study provides the first detailed data on how small insects, such as fruit flies, maintain stable flight when passing through thermal convection cells. The results suggest that small insects flying into thermal plumes can experience serious losses of flight control and may fall out of these plumes, with potentially negative consequences. This could significantly diminish the dispersal range of some species, especially for individuals and species with low aerodynamic capacities, like aphids, midges or thrips. Furthermore, our results suggest that thermal convection poses a significant challenge in terms of flight control and energetics to insects that frequently fly near surfaces heated by solar radiation and/or fermentation (e.g. fruit flies and other insects that feed on fermenting matter), as well as possibly hematophagous arthropods (e.g. mosquitoes) [38], which seek out and feed on warm-blooded hosts.

Data accessibility. This article has no additional data.

Authors' contributions. V.M.O.-J. conceived the idea. V.M.O.-J. and S.A.C. designed the experiments. V.M.O.-J. performed the experiments. V.M.O.-J. and S.A.C. performed the data analysis. V.M.O.-J. and S.A.C. wrote the manuscript.

Competing interests. The authors declare no competing interests.

Funding. This work was supported by the National Science Foundation CAREER grant IOS-1253677 to S.A.C.

Acknowledgements. We want to thank Martin Hauser for his help in fruit fly identification and to Ukyong Chang for her help with video digitization.

References

1. Bodenschatz E, Pesch W, Ahlers G. 2000 Recent developments in Rayleigh-Bénard convection. *Annu. Rev. Fluid Mech.* **32**, 709–778. (doi:10.1146/annurev.fluid.32.1.709)
2. Czarnota T, Wagner C. 2011 Turbulent convection in a Rayleigh-Bénard cell with solid horizontal plates of finite conductivity. In *Direct and large-eddy simulation VIII* (eds H Kuerten, B Geurts, V Armenio, J Fröhlich). ERCOFTAC Series, vol. 15, pp. 371–376. Dordrecht, The Netherlands: Springer. (doi:10.1007/987-94-007-2482-2_59)
3. Chillà F, Schumacher J. 2012 New perspectives in turbulent Rayleigh–Bénard convection. *Eur. J. Phys. E* **35**, 58. (doi:10.1140/epje/i2012-12058-1)
4. Mildrexler DJ, Zhao M, Running SW. 2011 Satellite finds highest land skin temperatures on Earth. *Bull. Am. Meteorol. Soc.* **92**, 855–860. (doi:10.1175/2011BAMS3067.1)
5. Garratt JR. 1992 Extreme maximum land surface temperatures. *J. Appl. Meteorol.* **31**, 1096–1105. (doi:10.1175/1520-0450(1992)031<1096:EMLST>2.0.CO;2)
6. Synnefa A, Santamouris M, Apostolakis K. 2007 On the development, optical properties and thermal performance of cool colored coatings for the urban environment. *Sol. Energy* **81**, 488–497. (doi:10.1016/j.solener.2006.08.005)
7. Ortega-Jimenez VM, Greeter JS, Mittal R, Hedrick TL. 2013 Hawkmoth flight stability in turbulent vortex streets. *J. Exp. Biol.* **216**, 4567–4579. (doi:10.1242/jeb.089672)
8. Ortega-Jimenez VM, Sapir N, Wolf M, Variano EA, Dudley R. 2014 Into turbulent air: size-dependent effects of von Kármán vortex streets on hummingbird flight kinematics and energetics. *Proc. R. Soc. B* **281**, 20140180. (doi:10.1098/rspb.2014.0180)
9. Ravi S, Crall J, Fisher A, Combes SA. 2013 Rolling with the flow: bumblebees flying in unsteady wakes. *J. Exp. Biol.* **216**, 4299–4309. (doi:10.1242/jeb.090845)
10. Ortega-Jimenez VM, Mittal R, Hedrick TL. 2014 Hawkmoth flight performance in tornado-like whirlwind vortices. *Bioinsp. Biomim.* **9**, 025003. (doi:10.1088/1748-3182/9/2/025003)
11. Combes SA, Dudley R. 2009 Turbulence-driven instabilities limit insect flight performance. *Proc. Natl Acad. Sci. USA* **106**, 9105–9108. (doi:10.1073/pnas.0902186106)
12. Engels T, Kolomenskiy D, Schneider K, Lehmann FO, Sesterhenn J. 2016 Bumblebee flight in heavy turbulence. *Phys. Rev. Lett.* **116**, 028103. (doi:10.1103/PhysRevLett.116.028103)
13. Tucker VA. 1968 Respiratory exchange and evaporative water loss in the flying budgerigar. *J. Exp. Biol.* **48**, 67–87.
14. Vance T, Faruque I, Humbert JS. 2013 Kinematic strategies for mitigating gust perturbations in insects. *Bioinsp. Biomim.* **8**, 016004. (doi:10.1088/1748-3182/8/1/016004)
15. Weimerskirch H, Chastel O, Barbraud C, Tostain O. 2003 Frigatebirds ride high on thermals. *Nature* **421**, 333–334. (doi:10.1038/421333a)
16. Pennycuick CJ. 1983 Thermal soaring compared in three dissimilar tropical bird species, *Fregata magnificens*, *Pelecanus occidentalis* and *Coragyps atratus*. *J. Exp. Biol.* **102**, 307–325
17. Reynolds KV, Thomas ALR, Taylor GK. 2014 Wing tucks are a response to atmospheric turbulence in the soaring flight of the steppe eagle *Aquila*

nipalensis. *J. R. Soc. Interface* **11**, 20140645. (doi:10.1098/rsif.2014.0645)

18. Dickinson MH. 2014 Death valley, *Drosophila*, and the devonian toolkit. *Ann. Rev. Entomol.* **59**, 51–72. (doi:10.1146/annurev-ento-011613-162041)
19. Thielicke W, Stamhuis EJ. 2014 PIVlab—towards user-friendly, affordable and accurate digital particle image velocimetry in MATLAB. *J. Open Res. Softw.* **2**, e30. (doi:10.5334/jors.bl)
20. Hedrick TL. 2008 Software techniques for two- and three-dimensional kinematic measurements of biological and biomimetic systems. *Bioinspir. Biomim.* **3**, 034001. (doi:10.1088/1748-3182/3/3/034001)
21. Walker JA. 1998 Estimating velocities and accelerations of animal locomotion: a simulation experiment comparing numerical differentiation algorithms. *J. Exp. Biol.* **201**, 981–995.
22. R Development Core Team. 2013 *R: a language and environment for statistical computing*. Vienna, Austria: R Foundation for Statistical Computing. See http://www.R-project.org.
23. Marder J. 1973 Body temperature regulation in the brown necked raven (*Corvus corax ruficollis*). II. Thermal changes in the plumage of ravens exposed to solar radiation. *Comp. Biochem. Physiol. A: Physiol.* **45**, 431–440. (doi:10.1016/0300-9629(73)90450-7)
24. Crall JD, Chang JJ, Oppenheimer RL, Combes SA. 2017 Foraging in an unsteady world: bumblebee flight performance in field-realistic turbulence. *Interface Focus* **7**, 20160086. (doi:10.1098/rsfs.2016.0086)
25. Combes SA, Rundle DE, Iwasaki JM, Crall JD. 2012 Linking biomechanics and ecology through predator–prey interactions: flight performance of dragonflies and their prey. *J. Exp. Biol.* **215**, 903–913. (doi:10.1242/jeb.059394)
26. Kellermann V, van Heerwaarden B, Sgrò CM. 2018 How important is thermal history? Evidence for lasting effects of developmental temperature on upper thermal limits in *Drosophila melanogaster*. *Proc. R. Soc. B* **284**, 20170447. (doi:10.1098/rspb.2017.0447)
27. Ortega-Jimenez VM, Badger M, Wang H, Dudley R. 2016 Into rude air: hummingbird flight performance in unpredictable aerial environments. *Phil. Trans. R. Soc. B.* **371**, 20150387. (doi:10.1098/rstb.2015.0387)
28. Busse R, Hedenström A, Winter Y, Johansson LC. 2012 Kinematics and wing shape across flight speed in the bat, *Leptonycteris yerbabuenae*. *Biol. Open* **1**, 1226–1238. (doi:10.1242/bio.20122964)
29. Ristroph L, Ristroph G, Morozova S, Bergou AJ, Chang S, Guckenheimer J, Wang ZJ, Cohen I. 2013 Active and passive stabilization of body pitch in insect flight. *J. R. Soc. Interface* **10**, 20130237. (doi:10.1098/rsif.2013.0237)
30. Fisher A, Ravi S, Watkins S, Watmuff J, Wang C, Liu H, Petersen P. 2016 The gust-mitigating potential of flapping wings. *Bioinspir. Biomim.* **11**, 046010. (doi:10.1088/1748-3190/11/4/046010)
31. Dickinson MH, Lighton JRB. 1995 Muscle efficiency and elastic storage in the flight motor of *Drosophila*. *Science* **268**, 87–90. (doi:10.1126/science.7701346)
32. Lehmann F-O, Dickinson MH. 2001 The production of elevated flight force compromises manoeuvrability in the fruit fly *Drosophila melanogaster*. *J. Exp. Biol.* **204**, 627–635.
33. Liao JC, Beal DN, Lauder GV, Triantafyllou MS. 2003 Fish exploiting vortices decrease muscle activity. *Science* **302**, 1566–1569. (doi:10.1126/science.1088295)
34. Portugal SJ, Hubel TY, Fritz J, Heese S, Trobe D, Voelkl B, Hailes S, Wilson AM, Usherwood JR. 2014 Upwash exploitation and downwash avoidance by flap phasing in ibis formation flight. *Nature* **505**, 399–402. (doi:10.1038/nature12939)
35. Srygley RB, Thomas ALR. 2002 Unconventional lift-generating mechanisms in free-flying butterflies. *Nature* **420**, 660–664. (doi:10.1038/nature01223)
36. Geerts B, Miao Q. 2005 Airborne radar observations of the flight behaviour of small insects in the atmospheric convective boundary layer. *Environ. Entomol.* **34**, 361–377. (doi:10.1603/0046-225X-34.2.361)
37. Wainwright, CE, PM Stepanian, DR Reynolds, Reynolds AM. 2017 The movement of small insects in the convective boundary layer: linking patterns to processes. *Sci. Rep.* **7**, 5438. (doi:10.1038/s41598-017-04503-0)
38. Corfas RA, Vosshall LB. 2015 The cation channel TRPA1 tunes mosquito thermotaxis to host temperatures. *eLife* **4**, e11750. (doi:10.7554/eLife.11750)